Investigation of Carbon Monoxide Adsorption on Cationic Gold-Palladium Clusters

Yang-Mei Chen[a], Xiao-Yu Kuang[a], Xiao-Wei Sheng[a], Huai-Qian Wang[b], Peng Shao[a], and Min-Ming Zhong[a]

[a] Institute of Atomic and Molecular Physics, Sichuan University, Chengdu 610065, China
[b] College of Engineering, Huaqiao University, Quanzhou 362021, China

Reprint requests to X.-Y. K.; E-mail: scu_kxy@163.com

Density functional calculations have been performed for the carbon monoxide molecule adsorption on $Au_nPd_m^+$ ($n+m \leq 6$) clusters. In the process of CO adsorption, small Au clusters and Pd clusters tend to be an Au atom and three Pd atoms adsorption, respectively. For the mixed Au–Pd clusters, an Au atom, a Pd atom, two atoms consisted of an Au atom and a Pd atom, two Pd atoms, and three Pd atoms adsorption structures are displayed. The highest occupied molecular orbital–lowest unoccupied molecular orbital (HOMO–LUMO) gaps and natural bond orbital charge population are calculated. Moreover, CO adsorption energy, CO stretching frequency, and CO bond length (upon adsorption) are also analysed in detail. The results predict that the adsorption strength of Au clusters with CO and the C–O vibration strength is enhanced and reduced after doping of Pd in the $Au_nPd_mCO^+$ complexes, respectively.

Key words: Density Functional Calculations; $Au_nPd_m^+$ Clusters; CO Molecule.

1. Introduction

Transition bimetallic clusters have been utilized in technologically important areas ranging from catalysis [1 – 3] to optoelectronic [4], magnetic [5] and even medical applications [6]. These widespread applications are due to the rich diversity of compositions, structures, and properties of metallic alloys. Particularly, the impurity-doped gold clusters [6 – 13] always exhibit more favourable and typical aspects of chemical activities than their pure host metals. Among the candidate systems which have been investigated, the Au–Pd bimetallic clusters [7 – 13] attract more attentions because of their particular physical and chemical properties. Experimentally, Liu et al. [7] have characterized the system by transmission electron microscopy (TEM), X-ray diffraction (XRD), and X-ray photoelectron spectrometry (XPS) to illustrate the formation of bimetallic Au–Pd colloids. By anion photoelectron spectroscopy, Koyasu et al. [8] have also measured the electron affinities (EA) and the vertical detachment energies (VDE) for binary Au–Pd cluster anions. Theoretically, the geometric and electronic properties of neutral and charged Au_nPd ($n = 1 – 4$) clus-

ters [10] have been studied by use of density functional theory. Zanti andPeeters [11] have shown a continuous and logical evolution of structural, electronic, and energetic properties of bimetallic Pd_nAu_m clusters. However, to the best of our knowledge, there are very limited theoretical works on the detailed study for the cationic $Au_nPd_m^+$ ($n+m \leq 6$) clusters.

On the other hand, Au–Pd bimetallic nanoparticle catalysts exhibit good stability and excellent reactivity toward a number of chemical reactions, such as aromatics, hydrogenation, CO oxidation, and vinyl acetate synthesis [14 – 16]. In addition, the dopant atoms tend to decrease the reactivity of the pure gold clusters with CO for the $Ag_mAu_n^+$ and $Cu_mAu_n^+$ cluster [17 – 20]. But how does the dopant of palladium affect the reactivity of gold clusters with carbon monoxide? Furthermore, are their structures and properties greatly distinct from the pure cationic gold and palladium clusters? In order to explore further insight of carbon monoxide adsorption on Au–Pd clusters, we have investigated the evolutions of geometries, stabilities, and electronic properties of $Au_nPd_m^+$ clusters and their monocarbonyls. The aim of the present work is:

(i) to determine the most stable geometrical structures of the $Au_nPd_m^+$ ($n+m \leq 6$) clusters and their monocarbonyls;

(ii) to investigate the electronic properties of cluster without and with the adsorption of CO;

(iii) to explore the adsorption strength between $Au_nPd_m^+$ and CO.

2. Computational Details

Geometrical structures, together with the frequency analysis of the $Au_nPd_m^+$ clusters and their monocarbonyls are optimized with GAUSSIAN03 package [21]. For gold and palladium atoms, the full electron calculation is rather time-consuming, so the relativistic effective core potentials (RECP) [22, 23] are introduced. Then, the Stuttgart/Dresden double-zeta SDD [24, 25] basis set is adopted to describe the gold and palladium atoms in our calculation. The standard all-electron basis set $6-311+G$ (3df) is adopted for carbon and osxgen, which includes polarization and diffuse functions and gives a description for CO. The same methodology has been employed to study gold clusters and CO molecules [26, 27]. The combination of Becke's three-parameter hybrid functional incorporating the Perdew–Wang exchange and the correlation functional (B3PW91) [28−31] has also been used successfully for the gold-doped palladium cluster in our early literature [13]. Furthermore, we also list the several exchange-correlation functions tested on the Au_2, AuPd, and Pd_2 clusters in Table 1. The bond length (1.124 Å) and frequency (2222 cm^{-1}) of CO based on the B3PW91 functional and $6-311+G$ (3df) basis set

are in good agreement with the experimental values of 1.128 Å and 2143 cm^{-1} [34], respectively. Therefore, all the calculations are performed at the level of the B3PW91 method (SDD for Au and Pd atoms and $6-311+G$ (3df) for C and O) in this study.

In order to get the lowest energy structures of the $Au_nPd_m^+$ clusters and their monocarbonyls, a large number of initial structures are checked for each size. Vibrational frequency calculations are performed on all geometries, and we verify that all the frequencies are positive, indicating a local minimum energy configuration for both bare and CO-covered clusters. The adsorption energy of CO on the $Au_nPd_m^+$ cluster is calculated as $\Delta E_{ads} = E(CO) + E(Au_nPd_m^+) - E(Au_nPd_mCO^+)$. All energies are modified with the zero-point energy correction. Due to a fairly large basis set with diffuse and polarization functions on carbon and oxygen atoms, the natural bond orbital (NBO) charges might be more reliable than the Mulliken charges.

3. Results and Discussions

3.1. Geometries of the $Au_nPd_m^+$ Clusters and their Monocarbonyls

The ground state geometry is an important part in the field of cluster physics. Accordingly, we first study the ground state structures of the $Au_nPd_m^+$ ($n+m \leq 6$) and $Au_nPd_mCO^+$ ($n+m \leq 6$) clusters, which are shown in Figures 1 and 2. Their corresponding electronic states and symmertries (Sym) are all presented

Table 1. Ground-state properties of Au_2, AuPd, and Pd_2 based on different basis sets and density functionals, where the bond length (r) is in units of Å; the dissociation energy (D_e) is in units of eV.

Basis Set	Density Function	Au_2		AuPd		Pd_2	
		r	D_e	r	D_e	r	D_e
Lanl2dz	B3LYP	2.57	1.87	2.59	1.07	2.53	0.96
	B3PW91	2.55	1.90	2.56	1.00	2.50	0.92
	PW91P86	2.55	2.30	2.52	2.08	2.50	1.59
	PW91PW91	2.55	2.20	2.53	1.97	2.50	1.49
	PBEPBE	2.55	1.97	2.53	1.94	2.50	1.45
SDD	B3LYP	2.58	1.86	2.55	1.47	2.52	0.90
	B3PW91	**2.55**	**1.89**	**2.53**	**1.49**	**2.50**	**0.92**
	PW91P86	2.55	2.29	2.51	1.97	2.49	1.50
	PW91PW91	2.55	2.19	2.52	1.86	2.50	1.40
	PBEPBE	2.56	2.27	2.53	1.84	2.50	1.37
	Experiment	**2.47**[a]	**1.88**[a]	**2.30**[b]	**1.40**[c]	**2.48**[d]	**0.76**[d]

[a] See [9], [b] see [32], [c] see [33], [d] see [34].

Table 2. Calculated parameters of the ground-state of the $Au_nPd_m^+$ ($n+m \leq 6$) clusters and their monocarbonyls.

| Cluster | Bare metal cluster | | | M–CO Spin state | M–CO Sym | M–CO HOMO–LUMO gap (eV) | CO bond dist (Å) | CO freq (cm⁻¹) | CO charge |
	Spin state	Sym	HOMO–LUMO gap (eV)						
Au_2^+	$^2\Sigma_g$	$D_{\infty h}$	2.034	$^2\Sigma_g$	$C_{\infty v}$	2.746	1.117	2292	0.222
$AuPd^+$	$^1\Sigma_g$	$C_{\infty v}$	2.307	$^1\Sigma_g$	$C_{\infty v}$	2.973	1.118	2285	0.213
Pd_2^+	$^2\Sigma_u^1$	$D_{\infty h}$	2.789	$^2A'$	C_s	2.089	1.138	2098	−0.036
Au_3^+	A'	D_{3h}	4.031	$^1A_1$	C_{2v}	4.099	1.119	2274	0.215
Au_2Pd^+	$^2A'$	C_s	2.372	$^2A'$	C_s	2.749	1.119	2271	0.215
$AuPd_2^+$	$^3B_1$	C_{2v}	1.963	$^1A'$	C_s	2.963	1.152	2017	0.016
Pd_3^+	$^4A''$	C_s	1.918	$^2A_2$	C_{3v}	2.560	1.156	1976	−0.193
Au_4^+	$^2B_{1u}$	D_{2h}	1.427	$^2B_2$	C_{2v}	1.413	1.120	2257	0.227
Au_3Pd^+	$^1A_1$	C_{3v}	2.826	$^1A'$	C_s	3.340	1.143	2079	−0.008
$Au_2Pd_2^+$	$^2B_1$	C_{2v}	2.260	^2A	C_1	2.355	1.126	2209	0.191
$AuPd_3^+$	$^3A''$	C_s	1.719	$^3A''$	C_s	1.893	1.125	2214	0.237
Pd_4^+	$^4A_1$	T_d	2.868	^2A	C_1	1.877	1.170	1888	−0.145
Au_5^+	^1A_g	^1A_g	3.158	^1A	C_s	3.623	1.121	2254	0.208
Au_4Pd^+	$^2B_2$	C_{2v}	1.629	$^2A''$	C_s	1.702	1.122	2244	0.223
$Au_3Pd_2^+$	$^1A'$	D_{3h}	2.678	^1A	C_1	2.895	1.154	2004	−0.013
$Au_2Pd_3^+$	$^2B_2$	C_{2v}	1.799	^2A	C_1	2.306	1.150	2204	0.051
$AuPd_4^+$	$^3A_1$	C_{3v}	2.129	$^1A'$	C_s	1.965	1.175	1848	−0.102
Pd_5^+	$^4A'$	C_s	1.753	$2A''$	C_s	1.542	1.176	1840	−0.147
Au_6^+	$^2B_2$	C_{2v}	1.274	$^2A_1$	C_{2v}	1.380	1.122	2244	0.224
Au_5Pd^+	$^1A'$	C_s	2.376	$^1A'$	C_s	2.564	1.128	2193	0.252
$Au_4Pd_2^+$	^2A	C_1	2.048	^2A	C_1	1.913	1.129	2190	0.244
$Au_3Pd_3^+$	^3A	C_s	1.673	^1A	C_1	1.687	1.534	2004	0.061
$Au_2Pd_4^+$	$^2B_{1g}$	D_{4h}	1.634	$^2A_2$	C_{4v}	2.027	1.125	2222	0.500
$AuPd_5^+$	^3A	C_1	1.429	$3A''$	C_s	1.717	1.129	2185	0.185
Pd_6^+	^4A	C_1	1.416	$^2A_2$	C_{3v}	1.981	1.181	1810	−0.125

in Table 2. For the pure gold clusters with odd number of atoms, the spin state is a singlet, and it is a doublet otherwise. Due to a shrinking of the size of the s orbital and strong sd electron hybridization caused by the relativistic effect, Au_n^+ clusters tend to be planar structures. This is in consistent with reported literature [35]. In contrast, due to the weak sd electron hybridization, Pd_4^+, Pd_5^+, Pd_6^+, and the bimetallic $Au_nPd_m^+$ ($3 \leq n+m \leq 6$) clusters adopt three-dimensional structures. For the pure palladium clusters, their spin states are quartet except Pd_2^+. The mixed $Au_nPd_m^+$ ($n+m \leq 6$) clusters have the lowest spin multiplicity of singlet or doublet except for the $AuPd_2^+$, $AuPd_3^+$, $AuPd_4^+$, $AuPd_5^+$, and $Au_3Pd_3^+$ which are triplet. In addition, for mixed $Au_nPd_m^+$ with $n+m = 4$, 5, the ground state geometries are similar to each other. However, for $n+m = 6$, the ground state geometries with a same size are very different for different gold or palladium content. As an example, $Au_2Pd_4^+$ and $AuPd_5^+$ have octahedron ground state geometry, but the other six-atom clusters have irregular geometry. This complicate phe-

nomenon could be attributed to several effects, including relativistic effect of gold, charge transfer between gold and palladium, and atom size mismatch. The last effect leads to the tendency of forming more Au–Pd hetero-bonds, that could be the reason that the pure Au_2^+, Au_3^+, Pd_2^+, and Pd_3^+ clusters are planar, while mixed $Au_2Pd_2^+$, $Au_2Pd_3^+$, $Au_3Pd_2^+$, and $Au_3Pd_3^+$ clusters tend to be three-dimensional. This trend is similar to that observed in Au–Cu bimetallic cations [19].

Here we only enumerate the lowest-energy isomers for each size. In the process of CO adsorption, various adsorption sites including a gold atom, a palladium atom, two atoms being made up of a gold atom and a palladium atom, two palladium atoms, and three palladium atoms are displayed. Our optimized results show that a gold atom adsorption is the most favourable one in Au_nCO^+. The pure Au_nCO^+ complexes keep planar geometries except Au_5CO^+, and the Au_5^+ has the twisted X-shaped ground-state geometry after CO adsorption. These trends are consistent with the $Au_nCu_m^+$ clusters [19]. The most stable
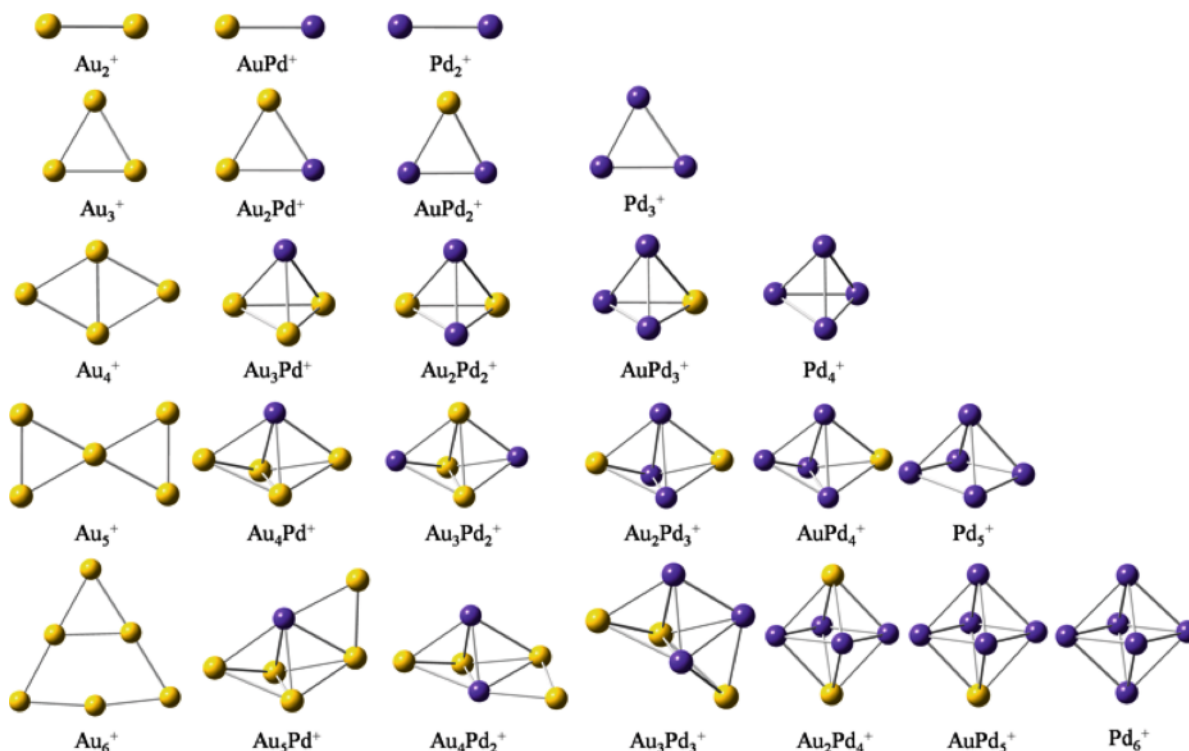
Fig. 1 (colour online). Optimized ground-state structures of the $Au_nPd_m^+$ ($n + m \leq 6$) clusters. The yellow and purple balls represent Au and Pd atoms, respectively.

structures of Pd_mCO^+ clusters are three-dimensional except Pd_2CO^+, and their spin states are doublet. In our calculations, the three palladium atoms adsorption structure is energetically more favoured for the pure Pd_mCO^+ complexes. This is possible due to that the $2\pi^*$ orbitals of CO interacting with the surface electrons at the hollow site is stronger. This behaviour is similar to previous studies [36]. In addition, the optimized ground state geometries indicate that the bimetallic $Au_nPd_mCO^+$ complexes have a gold atom, a palladium atom, and two atoms consisted of a gold atom and a palladium atom adsorption structures except $AuPd_4CO^+$ which is a three palladium atoms adsorption. The gold atom adsorption structures are displayed in $AuPdCO^+$, Au_2PdCO^+, Au_4PdCO^+, and $Au_2Pd_4CO^+$. While $Au_2Pd_2CO^+$, $AuPd_3CO^+$, Au_5PdCO^+, and $Au_4Pd_2CO^+$ have a palladium atom adsorption structure. The two palladium atoms adsorption structure is favourable in $AuPd_2CO^+$, $Au_3Pd_2CO^+$, $Au_2Pd_3CO^+$, and $Au_3Pd_3CO^+$. However, for the Au_3Pd^+ cluster, the CO is adsorbed between a gold atom and a palladium atom but the bond

length of Pd–C (1.87 Å) is smaller than the bond length of Au–C (2.15 Å).

3.2. Electronic Properties

In order to characterize the electronic structure of the considered clusters, the energy gap between the highest occupied molecular orbital (HOMO) and the lowest unoccupied molecular orbital (LUMO) has been investigated. The HOMO–LUMO energy gap reflects the ability for electrons to jump from the occupied orbital to the unoccupied orbital and represents the ability of the molecule to participate in chemical reactions to some degree. From a catalytic perspective, systems with smaller HOMO–LUMO gaps tend to be more reactive. In Table 2, we present the HOMO–LUMO gap for the clusters studied here, both without and with adsorbed CO. The results indicate that $Au_nPd_m^+$ have smaller HOMO–LUMO energy gaps than their monocarbonyls except Pd_2^+, Au_4^+, Pd_4^+, $AuPd_4^+$, Pd_5^+, and $Au_4Pd_2^+$. Therefore, it can be concluded that the cluster monocarbonyls are more
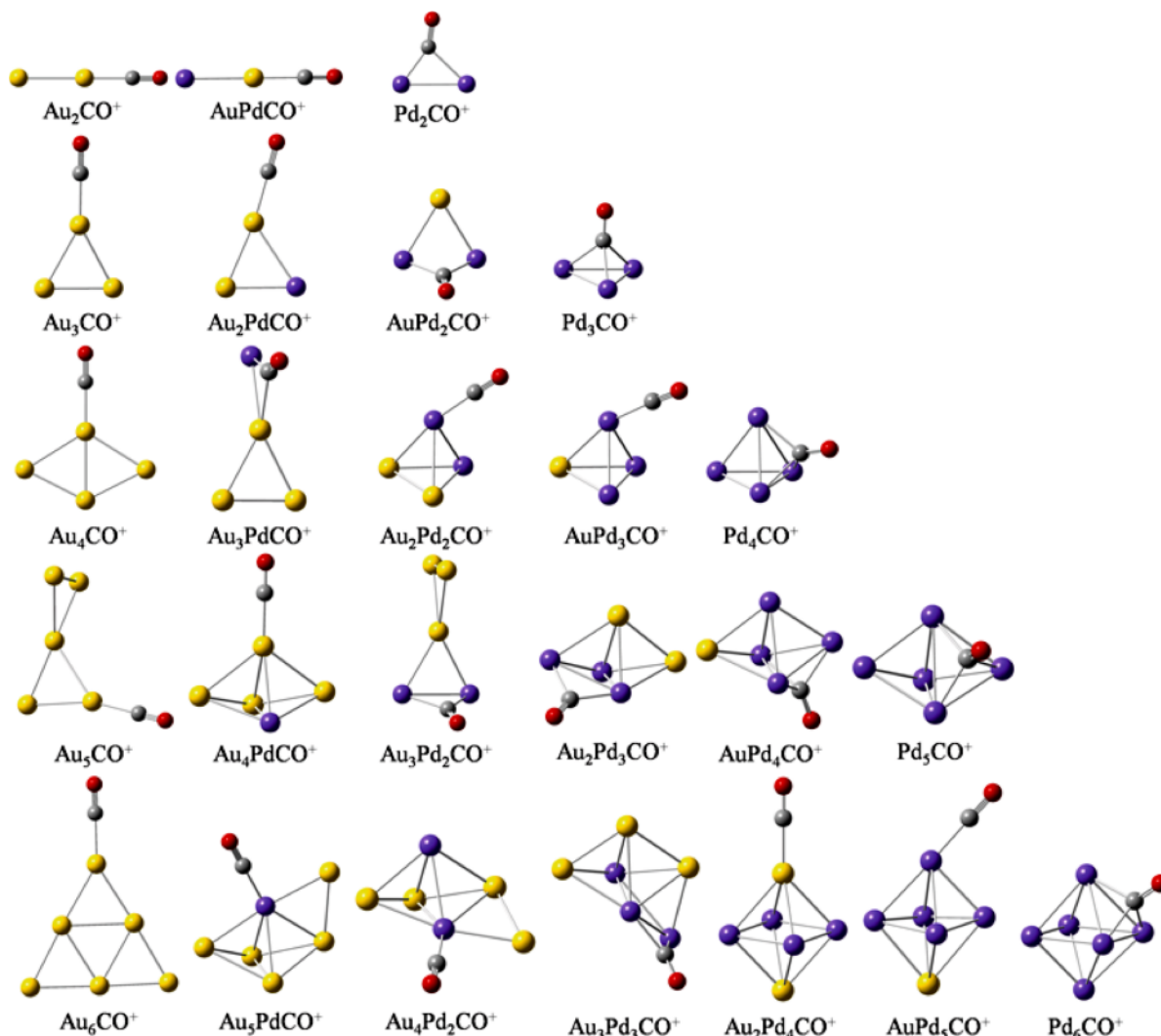
Fig. 2 (colour online). Optimized ground-state structures of the $Au_nPd_mCO^+$ ($n + m \leq 6$) complexes. The yellow, purple, gray, and red balls represent Au, Pd, C, and O atoms, respectively.

stable in chemical reactions than the clusters except Pd_2CO^+, Au_4CO^+, Pd_4CO^+, $AuPd_4CO^+$, Pd_5CO^+, and $Au_4Pd_2CO^+$. Besides, it is worth pointing out that larger HOMO–LUMO energy gaps for Au_4CO^+ and Pd_2CO^+ than Au_4^+ and Pd_2^+ may lead to that the HOMO–LUMO energy gap of $Au_4Pd_2CO^+$ is larger than that of $Au_4Pd_2^+$. In addition, the maximum value of HOMO–LUMO gap in pure Au_n^+, mixed $Au_nPd_m^+$, and pure Pd_m^+ clusters are 4.03 eV (Au_3^+), 2.83 eV (Au_3Pd^+), and 2.60 eV (Pd_4^+), respectively. Their monocarbonyls also have the largest

HOMO–LUMO gap value of 4.10 eV, 3.34 eV, and 2.86 eV in Au_nCO^+, bimetallic $Au_nPd_mCO^+$, and Pd_mCO^+.

Charge transfer is also an important quantity for studying the interaction between CO and the Au–Pd clusters. The natural bond orbital (NBO) charge population for adsorbed CO has been presented in Table 2. For the Au_n^+ clusters, the NBO charge population on adsorbed CO is positive, and the NBO charge on gold atoms has a decreasing trend after CO adsorption. This means that electron density flows from CO to the Au_n^+
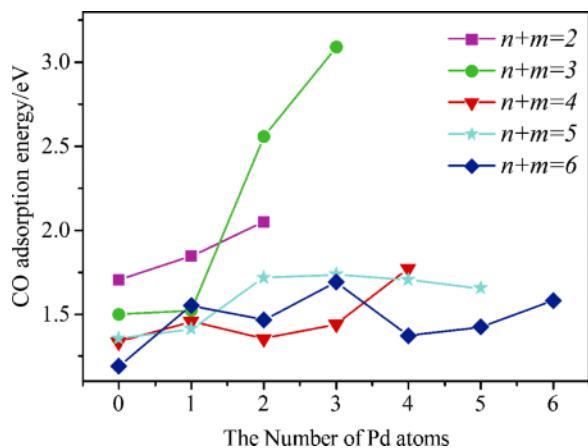
Fig. 3 (colour online). CO adsorption energy versus the contents of Pd atoms for clusters with different sizes.

cluster. On the contrary, the Pd_mCO^+ complexes show negative CO charge population and the Pd_m^+ clusters have increasing trend for the NBO charge on palladium atoms after CO adsorption. This indicates that electron density flows from the Pd_m^+ clusters to CO. The NBO charge population of the gold or palladium atoms in the bimetallic $Au_nPd_m^+$ clusters and their monocarbonyls are different. It is very hard for us to draw any interesting conclusion from the calculations. We only find that the NBO charge population on CO is positive for all the bimetallic $Au_nPd_mCO^+$ complexes except Au_3PdCO^+, $Au_3Pd_2CO^+$, and Au_4PdCO^+. These exceptions show that the electron density flows from Au_3Pd^+, $Au_3Pd_2^+$, and Au_4Pd^+ to CO.

3.3. Adsorption Strength of CO and C–O Vibration Strength

To evaluate the adsorption strength of the $Au_nPd_m^+$ clusters to the CO molecule, we calculate the adsorption energies of CO on the $Au_nPd_m^+$ clusters. As shown in Figure 3, when $n+m=2$, 3, the adsorption energy increases along with increasing palladium content, while for $n+m=4$, 5, there are weak increasing trends of the adsorption energy with the increasing palladium content. For the case of $n+m=6$, the increasing palladium content makes the adsorption energy show an odd-even oscillation except for $AuPd_5CO^+$. Overall, the reactivity of gold clusters with CO was found to be enhanced after dopant of palladium in the $Au_nPd_mCO^+$ complexes.

Moreover, the C–O stretching frequency and C–O bond length in $Au_nPd_mCO^+$ complexes are also presented. As shown in Table 2, compared with the values of free CO (2224 cm^{-1} and 1.124 Å), the C–O frequency in pure Au_nCO^+ complexes is increasing while the C–O bond length is reduced. The detailed analysis for C–O frequency and C–O bond length in the mixed $Au_nPd_mCO^+$ complexes expresses as follows: for $n+m=2$, 3, C–O frequency and bond length decreases and increases with increasing palladium content, respectively. When $n+m=4$, except $Au_2Pd_2CO^+$ and $AuPd_3CO^+$, the behaviour of C–O frequency and bond length is similar to complexes with $n+m=2$, 3. In the case of $n+m=5$, except $Au_2Pd_3CO^+$, there are decreasing and increasing trends for C–O frequency and C–O bond length. For $n+m=6$, except $Au_2Pd_4CO^+$ and $AuPd_5CO^+$, the similar behaviour to the case of $n+m=5$ for C–O frequency and bond length is also presented. In general, the strength of C–O vibration will decrease with increasing palladium content in $Au_nPd_mCO^+$ complexes.

4. Conclusions

Based on the density functional theory (DFT) approach, the geometries, stabilities, and electronic properties of the $Au_nPd_m^+$ clusters and their monocarbonyls have been systematically studied. The main conclusions are summarized as follows:

(i) The DFT calculations reveal that the most stable isomers for Au_n^+ are the planar structures when $n=1-6$. However, for the lowest energy structures of mixed $Au_nPd_m^+$ and Pd_m^+, the two- to three-dimension transition occurs at $n+m=4$. In the process of CO adsorption, pure gold clusters and pure palladium clusters tend to be a gold atom adsorption and three palladium atoms adsorption, respectively. For the mixed Au–Pd clusters, a gold atom, a palladium atom, two atoms consisted of a gold atom and a palladium atom, two palladium atoms, and three palladium atoms adsorption structures are displayed.

(ii) By comparing the HOMO–LUMO gap of the $Au_nPd_m^+$ clusters with their monocarbonyls, it can be predicted that the cluster monocarbonyls are more stable in chemical reactions than the bare clusters except Pd_2CO^+, Au_4CO^+, Pd_4CO^+, $AuPd_4CO^+$, Pd_5CO^+, and $Au_4Pd_2CO^+$. In addition, the NBO charge on adsorbed CO is

positive for the $Au_nPd_mCO^+$ complexes except Au_3PdCO^+, $Au_3Pd_2CO^+$, and Au_4PdCO^+ and pure Pd_mCO^+. This indicates that CO donate electrons to the $Au_nPd_m^+$ clusters except Au_3Pd^+, $Au_3Pd_2^+$, Au_4Pd^+, and pure Pd_m^+.

(iii) The adsorption strength of gold clusters with CO and C–O vibration strength is enhanced and reduced after dopant of palladium in the $Au_nPd_mCO^+$ complexes.

[1] J. W. A. Sachtler, J. P. Bibérian, and G. A. Somorjai, Surf. Sci. **110**, 43 (1981).

[2] C. Burda, X. B. Chen, and R. Narayanan, Chem. Rev. **105**, 1025 (2005).

[3] A. E. Russell and A. Rose, Chem. Rev. **104**, 4613 (2004).

[4] J. H. Hodak, A. Henglein, M. Giersig, and G. V. Hartland, J. Phys. Chem. B **104**, 11708 (2000).

[5] S. Y. Yin, X. S. Xu, and R. Moro, Phys. Rev. B **72**, 174410 (2005).

[6] N. L. Rosi and C. A. Mirkin, Chem. Rev. **105**, 1547 (2005).

[7] H. Liu, G. Mao, and S. Meng, J. Mol. Catal. **74**, 275 (1992).

[8] K. Koyasu, M. Mitsui, A. Nakajima, and K. Kaya, Chem. Phys. Lett. **358**, 224 (2002).

[9] K. Koyasu, Y. Naono, and M. Akutsu, Chem. Phys. Lett. **428**, 62 (2006).

[10] Z. J. Wu, S. H. Zhou, J. S. Shi, and S. Y. Zhang, Chem. Phys. Lett. **368**, 153 (2003).

[11] G. Zanti and D. Peeters, J. Phys. Chem. A **114**, 10345 (2010).

[12] B. R. Sahu, G. Maofa, and L. Kleinman, Phys. Rev. B **67**, 115420 (2003).

[13] A. J. Mao, X. Y. Kuang, G. Chen, and Y. R. Zhao, Mol. Phys. **109**, 1485 (2011).

[14] B. Pawelec, A. Venezia, V. L. Parola, E. Cano-Serrano, J. Campos-Martin, and J. Fierro, Appl. Surf. Sci. **242**, 380 (2005).

[15] R. W. J. Scott, C. Sivadinarayana, and O. M. Wilson, J. Am. Chem. Soc. **127**, 1380 (2005).

[16] S. L. Peng, L. Y. Gan, and R. Y. Tian, Comput. Theo. Chem. **977**, 62 (2011).

[17] M. Neumaier, F. Weigend, O. Hampe, and M. M. Kappes, J. Chem. Phys. **125**, 104308 (2006).

[18] M. Neumaier, F. Weigend, O. Hampe, and M. M. Kappes, Farad. Disc. **138**, 393 (2008).

[19] Y. Zhao, Z. Y. Li, and J. L. Yang, Phys. Chem. Chem. Phys. **11**, 2329 (2009).

[20] A. M. Joshi, M. H. Tucker, W. N. Delgass, and K. T. Thomson, J. Chem. Phys. **125**, 194707 (2006).

[21] M. J. Frisch, G. W. Trucks, H. B. Schlegel, G. E. Scuseria, M. A. Robb, J. R. Cheeseman, J. A. Montgomery, Jr., T. Vreven, K. N. Kudin, J. C. Burant, J. M. Millam, S. S. Iyengar, J. Tomasi, V. Barone, B. Mennucci, M. Cossi, G. Scalmani, N. Rega, G. A. Petersson, H. Nakatsuji, M. Hada, M. Ehara, K. Toyota, R. Fukuda, J. Hasegawa, M. Ishida, T. Nakajima, Y. Honda, O. Kitao, H. Nakai, M. Klene, X. Li, J. E. Knox, H. P. Hratchian, J. B. Cross, V. Bakken, C. Adamo, J. Jaramillo, R. Gomperts, R. E. Stratmann, O. Yazyev, A. J. Austin, R. Cammi, C. Pomelli, J. Ochterski, P. Y. Ayala, K. Morokuma, G. A. Voth, P. Salvador, J. J. Dannenberg, V. G. Zakrzewski, S. Dapprich, A. D. Daniels, M. C. Strain, O. Farkas, D. K. Malick, A. D. Rabuck, K. Raghavachari, J. B. Foresman, J. V. Ortiz, Q. Cui, A. G. Baboul, S. Clifford, J. Cioslowski, B. B. Stefanov, G. Liu, A. Liashenko, P. Piskorz, I. Komaromi, R. L. Martin, D. J. Fox, T. Keith, M. A. Al-Laham, C. Y. Peng, A. Nanayakkara, M. Challacombe, P. M. W. Gill, B. G. Johnson, W. Chen, M. W. Wong, C. Gonzalez and J. A. Pople, GAUSSIAN 03 (Revision A.1), Gaussian, Inc., Wallingford, CT 2004.

[22] P. J. Hay and W. R. Wadt, J. Chem. Phys. **82**, 299 (1985).

[23] C. M. M. Rohlfing and P. Jeffrey Hay, J. Chem. Phys. **83**, 4641 (1985).

[24] M. Dolg, U. Wedig, H. Stoll, and H. Preuss, J. Chem. Phys. **86**, 886 (1987).

[25] P. Schwerdtfeger, M. Dolg, W. H. E. Schwarz, and G. A. Bowmaker, J. Chem. Phys. **91**, 1762 (1989).

[26] X. Ding, Z. Li, J. Yang, J. G. Hou, and Q. Zhu, J. Chem. Phys. **120**, 9594 (2004).

[27] X. Ding, Z. Li, J. Yang, J. G. Hou, and Q. Zhu, J. Chem. Phys. **121**, 2558 (2004).

[28] A. D. Becke, Phys. Rev. A **38**, 3098 (1988).

[29] J. P. Perdew, J. A. Chevary, S. H. Vosko, A. J. Koblar, R. P. Mark, D. J. Singh, and C. Fiolhais, Phys. Rev. B **46**, 6671 (1992).

[30] J. P. Perdew, J. A. Chevary, S. H. Vosko, A. J. Koblar, R. P. Mark, D. J. Singh, and C. Fiolhais, Phys. Rev. B **48**, 4978 (1993).

[31] J. P. Perdew, K. Burke, and Y. Yang, Phys. Rev. B **54**, 16533 (1996).

[32] I. Efremenko and M. Sheintuch, Surf. Sci. **414**, 148 (1998).

[33] R. C. Weast, CRC Handbook of Chemistry and Physics, 65th ed. CRC Press, Boca Raton 1984.

[34] K. P. Huber and G. Herzberg, Constants of Diatomic Molecules, Van Nostrand Reinhold, New York 1979.

[35] S. Gilb, P. Weis, F. Furche, and R. Ahlrichs, J. Chem. Phys. **116**, 4094 (2002).

[36] B. Kalita and R. C. Deka, Eur. Phys. J. D **53**, 51 (2009).